Rock and Soil Mechanics

Volume 42 | Issue 1 Article 7

5-26-2021

Field measurement and numerical analysis for evaluating longitudinal settlement induced by shield tunneling parallel to building

Xuan DAI
College of Airport Engineering, Civil Aviation University of China, Tianjin 300300, China

Wang GUO
Tianjin Municipal Engineering Design and Research Institute, Tianjin 300392, China

Xue-song CHENG
MOE Key Laboratory of Coast Civil Structure Safety, Tianjin University, Tianjin 300072, China

Hai-feng HUO
College of Airport Engineering, Civil Aviation University of China, Tianjin 300300, China

See next page for additional authors

Custom Citation

DAI Xuan, GUO Wang, CHENG Xue-song, HUO Hai-feng, LIU Guo-guang, . Field measurement and numerical analysis for evaluating longitudinal settlement induced by shield tunneling parallel to building[J]. Rock and Soil Mechanics, 2021, 42(1): 233-244.

Field measurement and numerical analysis for evaluating longitudinal settlement induced by shield tunneling parallel to building

Authors

Xuan DAI, Wang GUO, Xue-song CHENG, Hai-feng HUO, and Guo-guang LIU

Rock and Soil Mechanics 2021 42(1): 233–244 ISSN 1000–7598
https: //doi.org/10.16285/j.rsm.2020.5763 rocksoilmech.researchcommons.org/journal

Field measurement and numerical analysis for evaluating longitudinal settlement induced by shield tunneling parallel to building

DAI Xuan[1], GUO Wang[2], CHENG Xue-song[3], HUO Hai-feng[1], LIU Guo-guang[1]

1. College of Airport Engineering, Civil Aviation University of China, Tianjin 300300, China
2. Tianjin Municipal Engineering Design and Research Institute, Tianjin 300392, China
3. MOE Key Laboratory of Coast Civil Structure Safety, Tianjin University, Tianjin 300072, China

Abstract: The transverse settlement induced by the construction of a parallel shield tunnel alongside the building has raised considerable attention, whereas few studies focus on the longitudinal settlement. Therefore, the spatial deformation of ground developed from this tunneling form is investigated. In this study, some field measurements from the shield tunnel section of Tianjin Metro Line 6 parallel to four similar masonry buildings in vicinity are analyzed first, and the deformation pattern is established. Then, a hardening soil model calibrated against field measurement, considering small strain stiffness, is implemented in a three-dimension finite element simulation to evaluate the longitudinal deflection of the buildings, the ground deformation, and the soil stress distribution. Additionally, the effect of building aspect ratio is discussed. The simulation results show that tunneling-induced sagging deformation develops along the longitudinal direction of the building, and the settlement at the middle of a longitudinal wall is twice of that at the corners. Therefore, the study of tunneling parallel to buildings cannot be simplified to a plane strain problem. The building construction and tunneling activity result in the soil above the tunnel crown experiencing a complicated stress history, which can be divided into six stages. In longitudinal direction, compared with the part below the building foundation corners, the soil in the middle initially behaves larger compressive deformation due to building construction, followed by greater unloading deformation caused by tunnel excavation. In addition, the longitudinal sagging is significantly reduced for the buildings with aspect ratio less than 2.

Keywords: shield tunneling; parallel tunneling; building settlement; finite element method (FEM); HS-Small model

1 Introduction

Shield tunneling is commonly applied in tunnel constructions in moderen city. Bacause of the limitation fo underground space, the undercrossing and parallel tunneling below exsting buildings are gradually a significant issue studied by a number of researchers[1−3]. To investigate the tunneling induced ground response, a lot of work using different methods, involving theoratical analysis[4], field meaurement[5], laboratory testing[6] and numerical simulation[7], has been carried out. The normal distribution curve introduced by Peck (1969)[8] based on large amount of engineering data is widely accepted for ground surface deformation analysis. In the above-mentioned research, due to the consistency of tunnel structure in length direction, the cross section of the tunnel is often intercepted and simplified as a plane strain problem for analysis[9]. The Peck equation, however, is merely focusing on the ground settlement after tunnelling, whilst ignoring the tunneling process. In fact, the deformation of ground surface develops in the direction of tunneling[1], as shown in Fig. 1. z_0 is the depth of tunnel axis; S_{max} represents for the maximum settlement; x, y, z are three axis in 3D space. Therefore, the ground deformation develops with tunneling progress, and consequently, the corresponding study on shield tunnel crossing buildings needs to be considered as a 3 dimension problem.

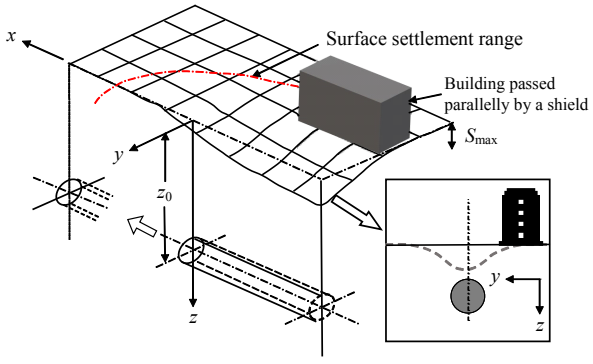

Fig. 1 Ground spatial deformation induced by tunneling[1]

In view of this issue, a number of 3D numerical models have been build up, concentrating on the variation of angle that the tunnel undercrosses (non parallel) the

Received: 5 June 2020 Revised: 22 September 2020
This work was supported by the National Natural Science Foundation of China (51808548), the Fundamental Research Funds for the Central Universities (3122018C017) and the Tianjin Technical Expert Project (20YDTPJC00750).
First author: DAI Xuan, male, born in 1988, PhD, Lecturer, mainly engaged in teaching and research in geotechnical engineering. E-mail: tianjindaixuan@126.com

building[10−11], so do the engineering reports available on field measurements [3, 12]. When the shield tunnel crosses non-parallel, the upper building will produce torsional deformation[13], which has a greater impact on deformation-sensitive buildings (such as masonry structures), so it has attracted more attention.When a tunnel is parallel to buildings, the attention that is mostly paid to is the transverse deformaiton (*yz* plane in Fig 1), and hence the problem is simplified to a 2D analysis [14]. However, the excavation of shield tunnel is progressing step by step, with obvious characteristics in spatial deformation development. In addition, the interaction between ground and foundation still takes place in the process of shield construction. Therefore, the simplified analysis method introduced above is not capable to summarise the longitudinal settlement regularities of buildings of the tunnel. Franzius[15] at Imperial College London pointed out the difference of ground loss among the stages of shield tunneling before reaching the building, during the crossing and after crossing. He also mentioned a certain deflection develops along the longitudinal direction of the building in the tunneling work. In fact, based on the analysis of measured data from a shield tunnel section of Tianjin Metro Line 6, the settlement of buildings along the longitudinal direction of the shield is found differential. Apparently, the longitudinal deformation of buildings is affected by the form of foundation, plane geometry, soil−foundation interaction and perhaps other factors, and hence a relevant special research is significant.

The statement above emphsizes that the impact on building settlement from different progressing stages and spatial factors. However, in terms of monitoring the impact of shield construction on buildings[16] and risk classification[17], corresponding codes in China are still mainly classfying them according to the distance between the building and the axis of the shield tunnel on the cross section view, whereas other factors are not taken into account.

To solve these problems, this paper firstly analyzes the measured settlement data of four brick-concrete buildings with similar aspect ratio and identical foundation forms in a section of Tianjin Metro Line 6 for summarizing the spatial deformation law of buildings caused by parallel shield tunneling. Then, on the basis of field measurements, a small strain hardening (HS-Small) is calibrated to characterize the small strain stiffness of the soil. The simulation is following realistic sequential excavation process and a 3D finite element model is built to analyze the influence on building settlement from the shield tunneling process. A series of stress paths is output to investigate the cause of building differential settlement in longitudinal direction. Finally, a sets of parametric analyses is carried out to study the influence of building aspect ratio on spatial deformation.

2 Site information and field measurement analysis

2.1 Site information

The tunnel section on Tianjin Metro Line 6 has a length of 508.99 m and 508.69 m in right and left lines, respectively, adopting single-circle single-line segment structure. Each tunnel ring has the outer diameter of 6200 mm, and the segments are 1500 mm in width and 350 mm in thickness. The twin tunnels have the interval between two axes is 16 m, buried at the depth of about 9.3−13.2 m. The soil layering, corresponding physical and mechanical properties of this site are shown in Table 1. The soil layer that the shield passes through in this section is mainly ⑥$_4$ silty clay layer. The groundwater level measured is about 1.4−2.0 m in depth during the period of site investigation.

The plan view of shield tunnel construction is shown in Fig. 2. The left line tunnel is excavated first, followed by the other one. In the range from ring number 150 to 320 in the left line, the parallel tunnel is successively excavated across four 6-storey brick-concrete buildings. The minimum clearance between No. 12 building and the tunnel is 7.6 m. The right line passes by a 6-storey heating center office building, and the minimum horizontal distance from the tunnel to the building is 8.2 m.

The basic information of the four residential buildings is shown in Table 2. The buildings, without deformation joints, are supported by raft foundations. Their aspect ratio on plane view is between 3.6 and 4.1. The environmental risk is ranked at grade 2. The monitoring risk is grade 2. In the process of shield tunneling, surface settlement, building settlement, segment settlement and settlement convergence are monitored. In simplicity, only building settlement measuring points are marked in Fig. 2. A total of 36 settlement measuring points are arranged on the buildings that is on left side of tunnel and parallel to the longitudinal direction of tunnel. Satisfying the technical requirements of national second-order leveling, the annexed leveling line is adopted, and all monitoring points are included.

https://rocksoilmech.researchcommons.org/journal/vol42/iss1/7
DOI: 10.16285/j.rsm.2020.5763

Table 1 Physical and mechanical properties of soil and the parameters for numerical simulation

Soil layers	Depths of bottom /m	γ /(kN • m^{-3})	c /kPa	φ /(°)	Parameters adopted in the analysis				
					G_0^{ref} / MPa	$\gamma_{0.7}$ /10^{-3}	E_{50}^{ref} /MPa	E_{oed}^{ref} / MPa	E_{ur}^{ref} / MPa
①$_1$Miscellaneous fill	3.2	14.0	2.2	10.2	70.96	0.2	4.38	4.38	26.28
④$_1$ Silty clay	5.5	19.6	15.7	15.4	165.06	0.2	18.34	18.34	55.02
⑥$_1$ Silty clay	7	19.2	17.4	19.3	173.43	0.2	19.27	19.27	57.81
⑥$_3$Silt	9	19.6	1.2	23.3	327.69	0.2	36.41	36.41	109.23
⑥$_4$ Silty clay	19	19.2	31.0	19.8	191.34	0.2	21.26	21.26	63.78
⑧$_2$ Silty sand	22	20.3	2.4	33.4	400.50	0.2	44.50	44.50	133.50
⑨$_1$ Silty clay	26	20.0	5.4	25.5	198.90	0.2	22.10	22.10	66.30
⑨$_2$ Silty sand	30	20.5	5.5	26.2	436.59	0.2	48.51	48.51	145.53

Note: γ is the soil unit weight; c is the cohesion; φ is the angle of internal friction; G_0^{ref} is the initial shearing modulus; $\gamma_{0.7}$ is the strain that the shearing modulus degrades to 70% of the initial value; E_{50}^{ref}, E_{oed}^{ref} and E_{ur}^{ref} are the secant stiffness in the standard drained triaxial test, the tangent stiffness for primary oedometer loading and the unloading/reloading stiffness from the drained triaxial test, respectively.

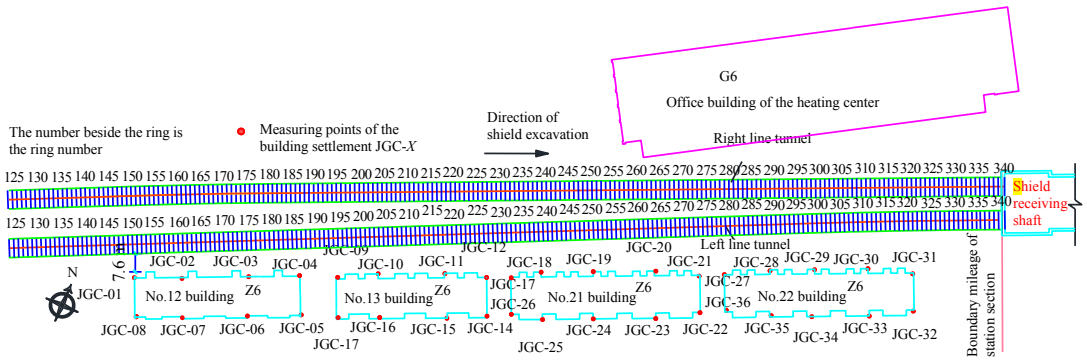

Fig. 2 Plan view of parallel tunneling alongside buildings

Table 2 Building information

Building No.	Size in plane	Structure form	Clearance from the tunnel /m
12	54 m×15 m	6-storey brick-concrete	7.6
13	49 m×15 m		9.0
21	62 m×15 m		10.0
22	62 m×15 m		11.4

2.2 Discussion on field measurements

In this project, the monitoring data among the buildings parallel to the tunnel are comparable due to the identical structure form, similar aspect ratio and clearance from the tunnel. The measured data of building settlement with tunnel ring number during shield tunneling is recorded in Fig. 3. Generally, the settlement induced by shield tunneling can be divided into five stages, involving initial settlement, settlement before tunnel face, shield passing-induced settlement, tail void-induced settlement and consolidation settlement. Those stages are reflected from the settlement development of buildings shown in Fig. 3. Before the shield machine reaches the building, due to the disturbance of the tunnel face pressure and other factors, the building develops the initial settlement and settlement before tunnel face. At these stages, the settlement values of the building are dominantly affected by the construction methods, and different pressure values in the pressure chamber leads to different settlement performances. For example, the settlement of building 12 is relatively small and the maximum settlement value for building 13 is only 4 mm, but a heaving behavior is observed on building 21 due to higher face pressure. When the shield tunnels beneath the building, the ground loss caused by the friction between the shield shell and the soil and the over-excavation of the shield cutter disc leads to the settlement of the building, and thus, synchronous grouting is often used to restricting the building settlement. Therefore, the settlement values of buildings at this stage are generally small. According to the measured results, the major settlement occurs after the shield crossing, and the process lasts for a long time. It can be seen from Figs. 3 (a) to (c) that the settlement of the building stops developing when the shield bores to ring 40 from the edge of the building, which implies that there is a certain lag effect of the building settlement with the excavation of the shield, and the monitoring of the building should be carried out until the deformation is stable. He et al.[14] reported the measured results of shield passing beneath the building, and it was found that the settlement of the building tended to be stable after the shield left the building for 60 m, which was consistent with the measured results in this paper.

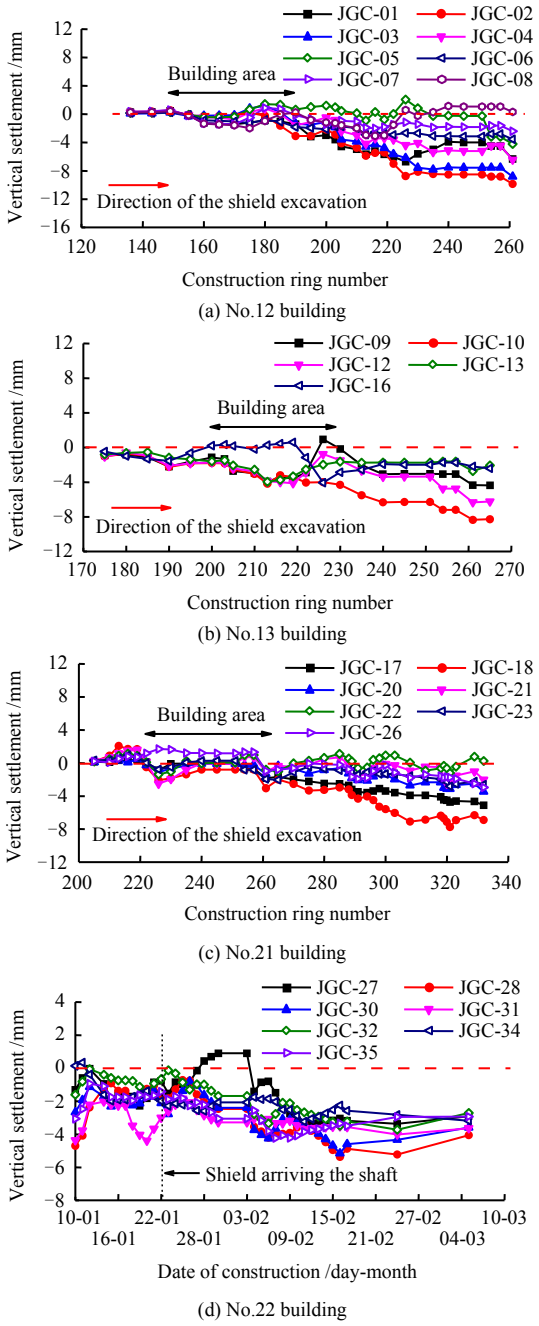

Fig. 3 Measured building settlement during tunneling

The lagging effect of building settlement is more obvious for building 22. The clearance between No. 22 building and the shaft is only 29 m. The monitoring work was still carried out after shield arriving. The data is shown in Fig.3 (d), in which the horizontal axis is the construction date. It is noted that the shield arrived the shaft at the date of 22 Jan., and some settlement of the building was already developing before this stage, especially for the JGC-31 measuring point, which is closer to the shaft, causing a settlement of 4.3 mm. The settlement reached stabilized 30 days after the shield arriving, and the values of that for No. 12, No. 13 and No. 21 buildings are about 8 mm, deemed consistent after the shield tunneling. Building No. 22 is closer to the shield shaft, and thus shield disturbance time is relatively short, so the maximum final settlement is 6 mm.

The longitudinal settlement (x-axis in Fig. 1) of a typical building developing with excavation time is shown in Fig. 4. Some variation of the settlement values along the longitudinal direction of the building can be found, showing in terms of small settlement on both ends and large settlement in the middle. Hence an obvious downward deflection is presented.

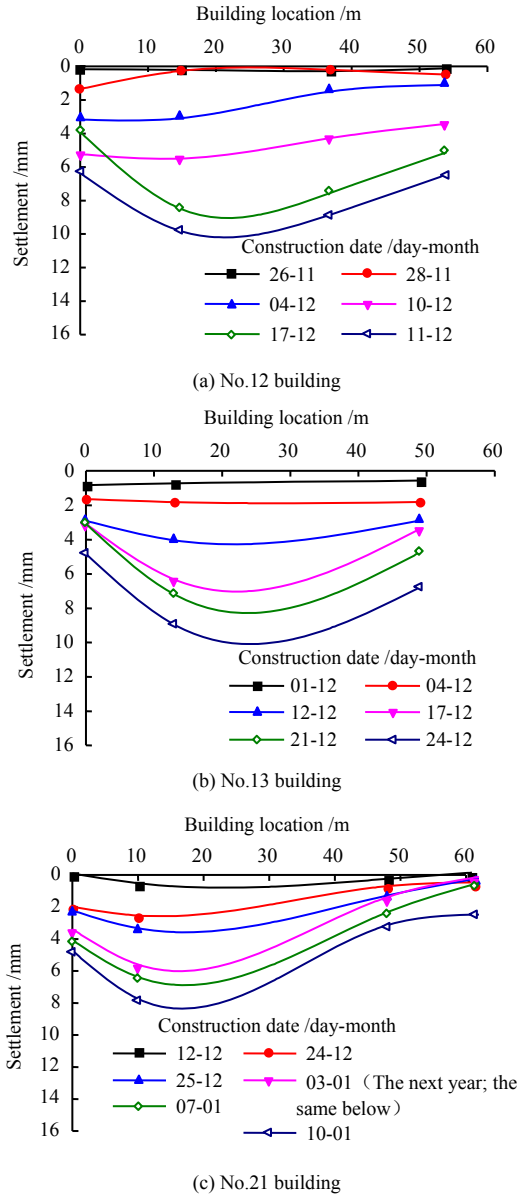

Fig. 4 Settlement of buildings in the longitudinal direction

The development of the longitudinal settlement of building 22 with the shield construction is plotted in Fig. 3 (d). The settlement values of the measuring points in the middle, such as JGC-28 and JGC-30, are larger than those of the edge measuring points (JGC-27 and JGC-31). After the shield crossing, similar longitudinal deflection deformation occurs as well. The settlement

of building 22 is affected by complex factors. On the one hand, building 22 has been disturbed by shield shaft construction at the beginning. On the other hand, the building is affected by shield crossing within a short time (shield arrives at the shaft with a short distance). Additionally, when the shield enters the shaft, the construction process such as the diaphragm wall breaking process will also affect its settlement.

In general, the concave deformation of the building is subsequently developing. It is highlighted that the concave deformation is not symmetrical, and consequently the building is inclined. In this project, the distance between buildings is small, and the settlement is not only affected by the shield, but also by the settlement of adjacent buildings. The deformation at the corners is especially paid attention to when monitoring is carried out. However, it can be interpreted from the analysis above that the corner deformation of building, crossed by shield beneath, does not represent the maximum deformation. The deformation measured from discrete points is not the maximum deformation either. Therefore, it is suggested that when the shield crosses beneath the building which are of large length width ratio, the measuring points set up at the middle position should be properly densified.

According to the code for design of building foundation (GB 5007−2011)[18], the local inclination control value of masonry bearing structure foundation is 0.002 for medium and low compressible soil. If the length of 10 m is taken, the settlement difference control value of the building is 20 mm. Although the local inclination of the building measured in this project has met the requirements of the code, the deflection deformation still occurred. Figure 5 shows the three-dimensional settlement diagram of the foundation of building 12 based on the measured data. *s* in the figure stands for the settlement value. It is noted that the foundation deformation is the superposition of inclined deformation and longitudinal deflection towards the shield construction direction. In this deformation mode, masonry buildings have the risk of shearing cracks. Since the building of this project adopted 400 mm thick raft foundation, which has smaller overall stiffness and larger aspect ratio, the deflection deformation is severe.

3 Construction of numerical analysis model

3.1 Modelling sequence and parametric study

A finite element numerical model has been constructed for further investigation on the spatial deformation of the buildings introduced above. The analysis was carried out on Plaxis^{3D}, and only the shield crossing No. 12 building was simulated in order to reduce the disturbance attributed from other factors. The discretization and the mesh built is shown in Fig. 6 below. The size of the mesh is of 150 m×70 m×30 m and is considered of proper scale to diminish the error caused by the mesh boundaries. Horizontal displacement is fixed on the mesh sides, whilst both horizontal and vertical components are fixed on the bottom. 10-noded triangular elements are adopted for the soil modelling, and the total number of the elements is 177680.

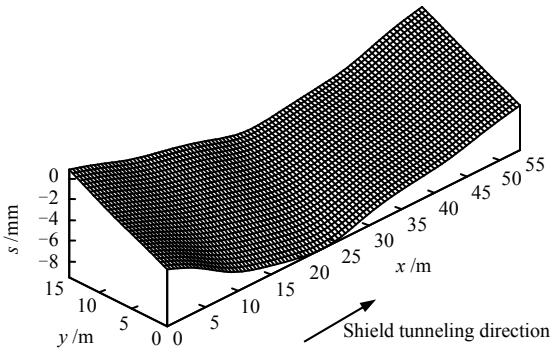

Fig. 5 Three-dimensional settlement diagram of building No. 12

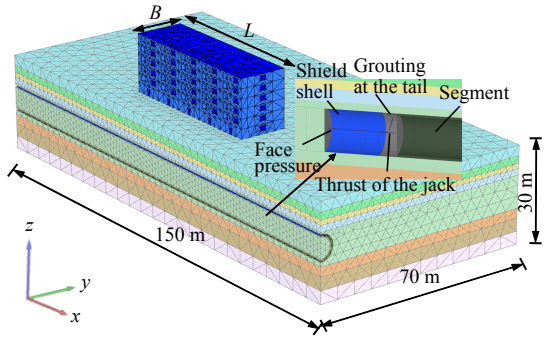

Fig. 6 Three-dimension finite-element simulation model

The side wall, floor and foundation of the building are simulated by plate element, and the corresponding design dead load and live load are imposed. In the process of simulation, the original building is simplified. The building is 6 stories each with the height of 3 m, and the doors and windows are open in the corresponding places. The thicknesses of the side wall, the floor and the foundation are 240 mm, 120 mm and 400 mm, respectively. The buried depth of foundation is 2 m. The distance between the building edge and the center of the shield tunnel is 11 m. The elastic moduli of floor and foundation are set as 30 GPa. In order to analyze the influence of different building plane aspect ratios, the building width *B* is defined as 15 m and the length *L* is 50 m, 40 m, 30 m, 20 m and 15 m, respectively in the parallel simulation.

A symmetrical semicircle is used to simulate the shield tunnel to achieve higher computational efficiency.

The buried depth at the crown of the tunnel is 10 m. Considering the shield construction process, the plate element is used to simulate the shield shell, and the shield body length is 9 m. The solid element is used to simulate the shield segment. The "birth and death element" is used to simulate the shield excavation, and the load is applied to simulate the face pressure, shield jacking force and shield tail grouting.

In the process of simulation, the first step is to achieve the ground stress equilibrium. Then the building construction is simulated to establish the corresponding stress field. Subsequently, the shield excavation is simulated. In this simulation, the segment width is 1.5 m. The calculation is carried out every two rings to simplify the simulation, so a total of 50 construction steps need to be simulated.

The simulation of shield tunneling are shown in Figs. 7 (a)−(e). Firstly, the soil in front of the shield machine is excavated, and the shield shell unit is activated to complete the forward movement of the shield machine. Meanwhile, according to the construction scheme, the tunnel face pressure of 160 kPa and shield tail grouting pressure of 200 kPa are applied in the model, followed with the generation of shield tail segment and the reloading of grouting pressure. According to the total jack thrust applying on the segment and the cross-sectional area, a jack pressure of 635.4 kPa is obtained. The ground loss, caused by shield tail gap, over-excavation of shield machine and some other factors, is simulated by interface shrinkage[3]. The value of ground loss η =1%, could be induced inversely from the measured data. This value is consistent with the statistical analysis results of ground loss ratio by Wei[19] and the recommendation. Therefore, the interface shrinkage ratio C is determined as 1%.

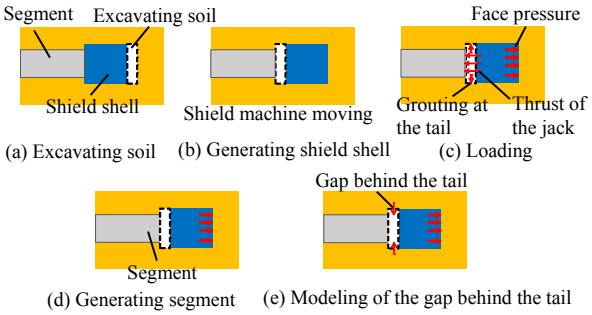

Fig. 7 Schematic of the tunneling procedure simulation

The large data set from the experiments has exposed that there is an important relationship between the stiffness of soil and its strain. Especially, under small strain condition, the stiffness of soil is significantly greater than that obtained from conventional test[20]. For general geotechnical engineering cases, the strain of soil is in the range of 0.01%−1.00%, as shown in Fig. 8. Without the consideration of small strain characteristics of soil, the deformation range of soil will be apparently overestimated for foundation pit excavation, tunnel excavation and other projects. Zheng et al.[21] and Lü et al.[22] have studied some cases of foundation pit engineering and tunnel engineering, etc. and highlighted that considering the small strain behavior of soil would be beneficial to describe the deformation of soil accurately. Therefore, the small strain hardening constitutive model (HS small model) is adopted to characterize the small strain behavior of soil via defining the initial shear modulus and degradation to 70% strain level. The soil parameters of numerical simulation are determined according to the results of laboratory tests, and the values are shown in Table 1.

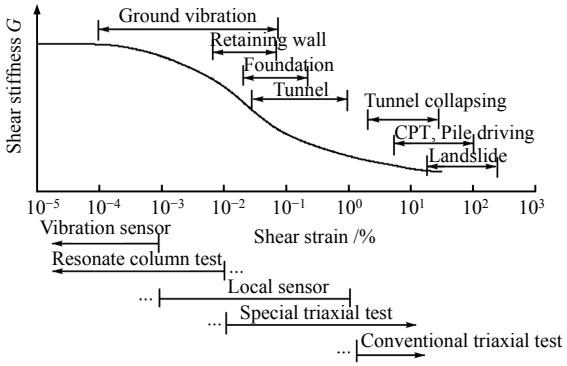

Fig. 8 Typical stiffness variation and strain ranges for different underground structures[23]

3.2 Verification of the model

The monitoring points of surface settlement trough are set up in the green field area of the shield tunneling. The results are compared with those of numerical simulation, from the stage in which the excavation has not reached the building area. In addition, the curves obtained by Peck formula[8] are also compared and analyzed. Peck formula is expressed as follows[8]:

$$S(y) = S_{\max} e^{-\frac{y^2}{2i^2}} \quad (1)$$

$$S_{\max} = \frac{V_s}{i\sqrt{2\pi}} = \frac{\pi R^2 \eta}{i\sqrt{2\pi}} \quad (2)$$

where $S(y)$ is the surface settlement at a certain position away from the central axis of the tunnel; $S_{\max}$ is the maximum settlement which usually occurs at the tunnel axis; i represents the coefficient of width of the settlement trough, also know as the distance from the inflection points to the tunnel center; R is the radius of the tunnel and V_s is the value of ground loss per linear meter.

Figure 9 shows the comparison of numerical simulation, engineering measurement and peck formula. The ground loss of peck formula in the figure is 1%, which is consistent

with the numerical simulation. It can be seen that the numerical simulation results are basically consistent with those of the peck formula and the measurements. Generally, the influence range of surface settlement is 4*D* (*D* is the tunnel diameter). In fact, there are a number of formulas for calculating the width coefficient *i* of surface settlement trough. Nevertheless, considering the characteristics of stratum division, a widely used formula [24] is adopted in this paper:

$$i = kz_0 \tag{3}$$

where *k* is the definition of the width parameter of the settlement trough. This value can be calculated according to the measured width of settlement trough and the depth of tunnel. The width coefficient *i* of settlement trough calculated by numerical simulation is $0.5z_0$, which is consistent with the recommended value for regional stratum characteristics in *Code for Monitoring Measurement of Urban Rail Transit Engineering* (GB 5911−2013) [16].

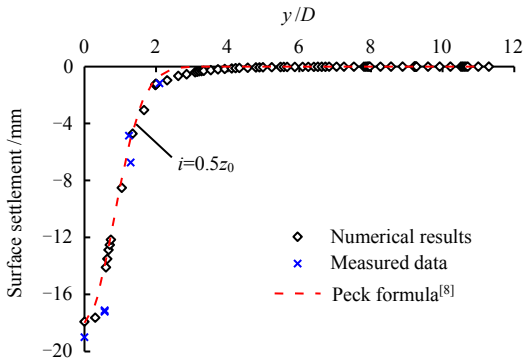

Fig. 9 Ground settlement induced by tunneling

Figure 10 shows the comparison results of the settlement values of JGC-02 measuring point. The settlement values of the numerical simulation and the measured results have good agreement, and the relative error is about 14%. However, the development process of settlement is slightly different. A lag could be found in the surface settlement values obtained from the measured results behind the numerical simulation results. This could be accounted for by the adoption of certain compensation grouting measures during shield construction and the "lag effect" mentioned above.

4 Numerical analysis results

4.1 Building settlement mode

In the process of shield tunneling, the settlement deformation of the bottom of the building longitudinal wall is shown in Fig.11, where *d* is the distance between the shield face and the building edge. It can be seen from Fig.11 (a) that the longitudinal settlement of the building (the shield side) changes with the shield tunneling. The building inclines to the excavation side due to ground disturbance when the shield face has not reached the building area. An inflection of this motion occurs when the shield face is close to the building center (*d*=28 m). A concave settlement mode in longitudinal direction is observed after the excavation crossing beneath the building, and this matches the performance measured (see Fig. 4(a)). Because of the large longitudinal length of the building and the thin foundation raft, the deformation it performs looks flexible. The building inclines longitudinally after the shield construction. Franzius[15] pointed out that the main reason for this inclination is that the ground loss rate before the shield arrives at the building is inconsistent with that under the building foundation. This explanation has good agreement with the calculation results in this paper.

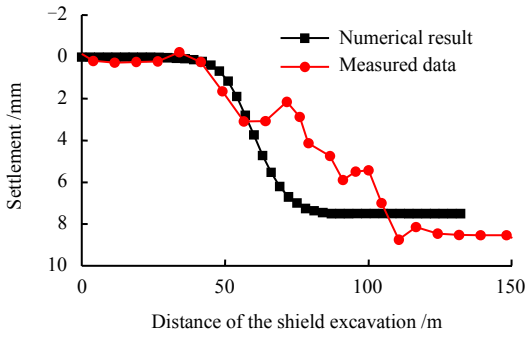

Fig. 10 Comparison of simulation and monitoring data of the JGC-02 settlement

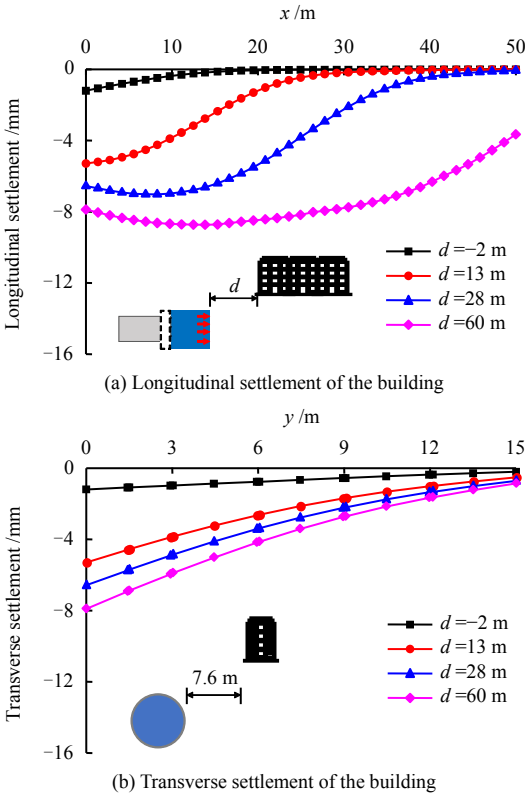

Fig. 11 Comparisons of longitudinal and transverse settlement patterns of building during tunneling

Figure 11 (b) shows the settlement of the bottom of the cross wall. The deformation is inclination based dominantly as the width of the foundation is short. The inclination degree is increasing with the excavation process. A slight "convex" deformation has also been observed in the building. According to the comparison of Fig. 11 (a) and Fig. 11 (b), for the case that shield passes beneath the building in parallel style, there is a great difference between the longitudinal deformation and the transverse deformation of the building.

In this project, the larger aspect ratio L/B of the building plane partly accounts for its longitudinal deflection. To evaluate the performance of longitudinal settlement of the shield passing beneath the building with large L/B and flexible foundation, the longitudinal settlement ratio is defined, which could be expressed as the fraction between the settlement value S_b at different positions of the bottom of the longitudinal wall and the settlement value S_{b0} at the corner of the longitudinal wall (choose the smaller magnitude of the two corners):

$$\delta=\frac{S_b}{S_{b0}} \tag{4}$$

The relative position α is defined as the ratio of the distance between the position of the longitudinal wall and the corner point which is influenced by tunnelling later (such as JGC-04 measuring point of No. 12 building) and the length L of the longitudinal wall. The relationship between the longitudinal settlement ratio and the relative position after the convergence of settlement is plotted in Fig.12, and the measured values are also shown in this figure. It can be found that the measured data and the numerical simulation results follow basically the same trend. This deviation of the longitudinal settlement ratio is decreasing with the shield excavation, and the maximum value can reach 2. The deflection of the building is not completely symmetrical. As the deformation of the building becomes stable, the deflection of the middle of the longitudinal wall tends to be gentle. In this simulation, the settlement of the corner of the longitudinal wall that the shield passes beneath first is 1.6 times that of the corner that the shield passes beneath later. In engineering practice, because of compensation grouting, stratum distribution and other factors, the actual deflection form of buildings will be more complicated. A polynomial is adopted to fit the longitudinal settlement ratio curve obtained from numerical simulation, and the formula is shown in Fig.12. The correlation coefficient R^2 = 0.985, showing good quality of this regression.

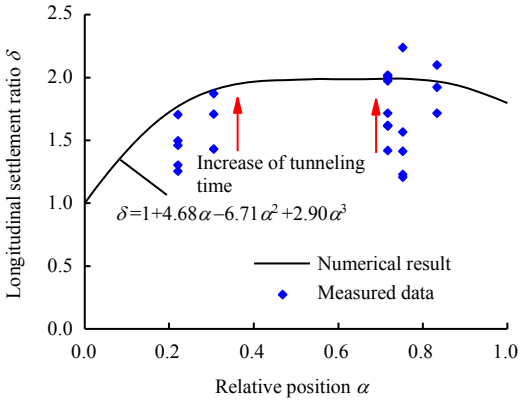

Fig. 12 Variations between longitudinal settlement ratio and the relative position

The deformation of buildings is of high relevance with the ground deformation, and inversely, the existence of buildings also affects the development of ground deformation. Figure 13 shows the settlement contour of the ground in the horizontal profile (3 m below the foundation bottom). The soil layer below the building is compressed during the building construction. The additional settlement caused by shield excavation could be found in this figure. Through the comparative analysis with the green field (such as the area with x =120−140 m in the figure), it is noted that the existence of buildings has an impact on the ground settlement. Under the green field condition, the ground settlement will be completely caused by the shield construction, and hence the contour line in the map should be basically staying horizontal and straight. However, the contour line has some deformation and distortion in the case with the influence of the building. The oval area in Fig.13 is the affected area of the deformation of the contour line of the ground settlement, which extends from the building foundation to the tunnel axis along the Y direction and exceeds the building foundation nearly 20 m along the X direction. Compared with green field condition, the vertical settlement of ground between tunnel axis and building foundation will decrease, while for the ground layers where building foundation is located, the vertical settlement value will increase. This behavior stated here is consistent with the conclusion of Potts et al.[25]. Obviously, the deformation difference mentioned above is related to the stress state and stress diffusion of the ground during the building construction. Therefore, the change of ground stress caused by the building construction should be considered for further analysis.

4.2 Stress analysis

Figure 14 shows the vertical stress diagram of the ground along the longitudinal direction of the building during tunnel excavation. Figure 14 (a) shows the state

when the building construction is completed, and the stress of the ground under the building foundation increases significantly.

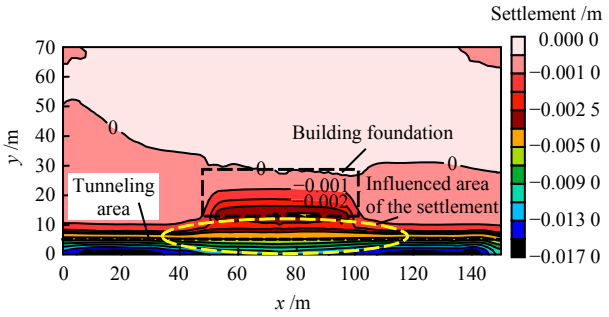

Fig. 13 Ground settlement contour map at horizontal profile

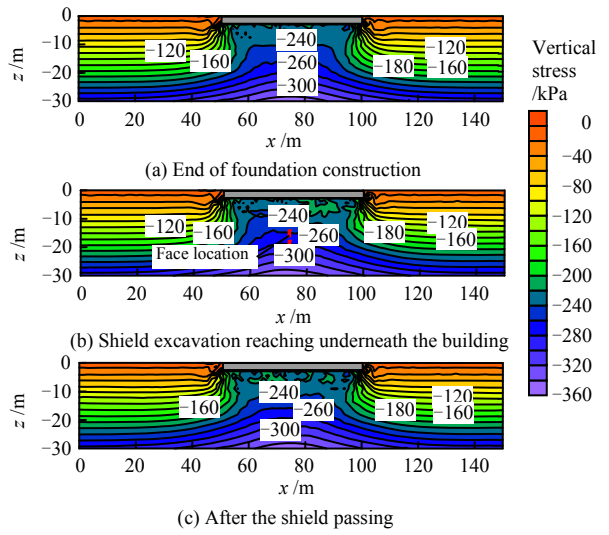

Fig. 14 Contour of the vertical stress of the ground during tunneling

As the shield tunneling is carried out under the foundation, the ground stress in the affected area will be reduced due to the ground loss. The zone of stress releasing appears in the shield shell and tail area. For the soil in front of the shield face, the internal stress increases with the negative earth pressure from the shield, as shown in Fig.14(b). In Fig.11, the settlement pattern developed by the building is related to the reduction of soil stress in this stage. After the shield crossing, a low stress zone will be formed underneath the foundation, as shown in Fig. 14(c). Compared with Fig. 14(b), the depth of the low stress zone is reduced, the ground stress recovers and the stress in the middle of the foundation is higher than that on both sides. Considering the interaction performance between building foundation and the ground, this project is a raft foundation with relatively small rigidity, which will initially produce "sag" deformation from the upper load. This interaction feature is still acting with the change of vertical stress during the shield excavation process. Specifically, with the ground loss the stress releasing taking place, the deformation of the foundation is still affected by the relative stiffness of the foundation, which further generates the tendency of "concaving" deformation.

The law of deformation and stress change of soil are accountable for each other, this relationship can be further explained with the following stress path. Figure 15 shows the data of vertical effective stress σ'_z against horizontal effective stress σ'_x of typical measuring points. The measuring points S1−S3, which are above the tunnel axis, are located at the center of the building foundation, the longitudinal edge of the foundation, and outside the influence range of the building foundation (green field), respectively. The following rules are exposed by analyzing the stress paths in the figures:

(1) The stress state of each measuring point can be divided into six stages (1−6 in Fig. 15) according to the diagram of stress path, and it seems complex due to the influence of building history and shield tunneling. The initial stresses of those points are located at the same point on the k_0 line regarding the identical buried depth. Stage 1 is the stage of building construction, in which the building load leads to the increase of the ground stress, and hence σ'_x and σ'_z are increasing. In stage 2, the shield face has not reached the measuring points but is producing pressure, which leads to the growth of the ground horizontal stress. Thus the σ'_x is increased obviously, whilst σ'_z is only increased by a small amount. In stage 3, the shield face is below the measuring point, and the stress of the measuring point is increased due to the thrust pressure. The increase of σ'_z at this stage is obvious, which could be related to the relative position between the shield face and the measuring point. The stress releases at the 4th stage as the shield passing causes the ground loss. Stage 5 is featured with the influence from the shield tail in terms of the grouting pressure and the gap, inducing a small rise of σ'_z. The stress recovery takes place at the 6th stage, when the shield has been detached from the measuring point and the soil tends to stabilize, and the vertical stress recovers gradually at the measuring point. Due to the friction between shield shell and soil, the final horizontal stress of soil increases. However, the final vertical stress of measuring point is less than its initial state, which could be explained with the ground loss. In fact, in long-term consolidation stage, σ'_z is supposed to increase gradually, combining with the settlement of soil and the building. In this model, however, the consolidation stage after tunneling is not studied.

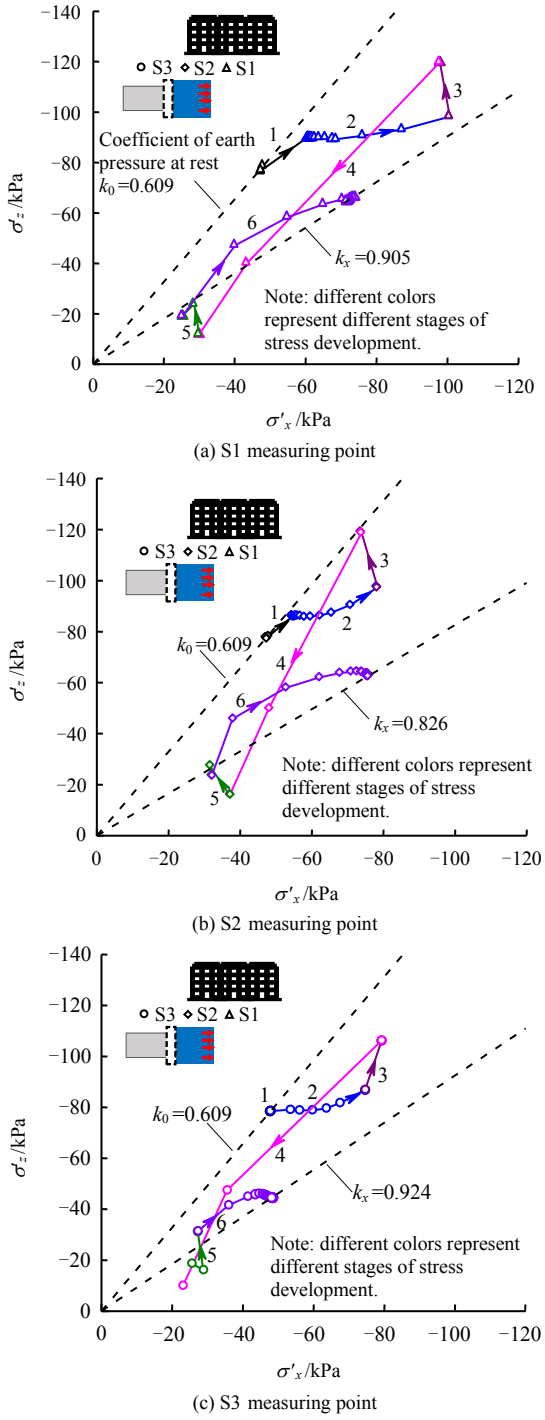

Fig. 15 Stress paths at different ground locations

(2) Comparing the stress paths of S1 and S2 in stage 1, the stress increase of S1 is significantly greater than that of S2 since the additional stress in the center of the foundation is higher than that at the edge. This stress deviation also leads to the "concave" deformation of the flexible foundation in the longitudinal direction. As for stage 2, the S1 is greatly constrained by the additional stress of foundation, and hence the higher horizontal stress is developed under the thrust of shield face. The building settlement during the shield excavation is mainly caused by the stress release. It can be found that the stress release degree of S1 measuring point is significantly greater than that of S2 measuring point, directly leading to the longitudinal deflection of the building after shield excavation. In stage 6, the deformation of the stratum does not change much despite the increase of the ground stress. This could be explained by the stress history of "loading (stages 1−3) − unloading (stage 4) −reloading (stages 5−6)", and the deformation of the soil at the moment is determined by the rebound−compression modulus. The horizontal stress ratio k_x of S1 is 0.905, which is slightly larger than that of S2.

In conclusion, the soil under the middle part of the foundation near the shield has undergone the compression deformation caused by the increase of additional stress under the action of building load. After the shield passes underneath, the soil has performed unloading deformation caused by stress releasing, resulting in the longitudinal "concave" deflection of the building.

(3) S3 measuring point is located outside the building area and is less affected by the building load, so there is no additional stress increase in stage 1. At the end of stage 3, the vertical stress is only about 80% of that of S1. This behavior also leads to the lower stress reduction of S3 when σ'_z is reduced to the same stress level in unloading process of stage 4, but the ground settlement at S3 is larger (S3 is located outside the settlement influence area in Fig.13). The reason is related to the deformation caused by stress recovery. Because S3 measuring point has not experienced loading stage, implying low over-consolidation ratio, a substantial deformation with low stress level will be developed in stage 6. Regarding the comparison between the initial state and final state, the vertical stress of S3 measuring point (outside the building influence area) has been reduced by 50%, while that of S1 and S2 measuring points has only been reduced by 25%.

4.3 Influence of building aspect ratio

The deformation mode of the building is affected by the foundation stiffness. The larger aspect ratio with thinner foundation results in lower resistance to the deformation, and it is easier to deflect in the longitudinal direction. The trial analyses of the aspect ratio of the building plane to 3.3, 2.7, 2.0 and 1.0 respectively have been carried out, investigating the relationship between the longitudinal settlement ratio and the relative position (the part with obvious deflection) under different length width ratios, as shown in Fig.16. The variation of the maximum longitudinal settlement ratio δ_{max} is also presented in this figure. The δ_{max} decreases by 30% when the aspect ratio decreases from 3.3 to 2.7 (by 18%), and this value is less than 1.3 when the latter is less than 2.0. This behavior indicates that the foundation stiffness is a more sensitive factor. In the case that the shield passes aside the building, which has a flexible foundation such as raft foundation and strip foundation

and high aspect ratio, in a parallel form, the monitoring quality of the deformation of the building longitudinal wall should be emphasized to prevent cracking caused by the longitudinal deflection.

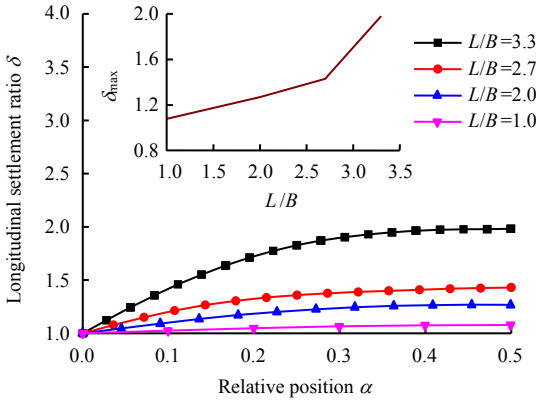

Fig. 16 Influence of building aspect ratio on longitudinal settlement ratio

Figure 17 shows the comparison of the longitudinal settlement when the shield face is excavated to the center of the building, and $\Delta x/L$ is the normalized vertical position of the building. The influence of the aspect ratio of the plane is also reflected from this figure. Since the time-spatial change of shield excavation has a great impact on the building settlement, when the building is excavated to the middle of the foundation, the longitudinal deflection of the building would be substantial. As for the building with aspect ratio less than 2.0, the longitudinal settlement of the building is small and linearly distributed. It is noteworthy that the interaction between foundation and foundation should be taken into account not only during the construction loading stage, but also during shield excavation since it determines the spatial deformation mode of foundation. Actually, the stiffness of building foundation is also affected by the thickness and type of foundation, and the stiffness of building also affects the unloading deformation mode of shield excavation. However, due to the constraints of this paper length, this information is not discussed in detail here.

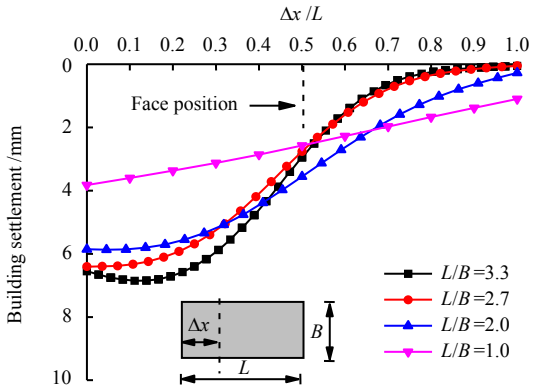

Fig. 17 Influence of building aspect ratio on longitudinal deflection during tunneling

5 Conclusion

In this paper, the measured data of four masonry buildings with identical structure, where the tunnel is excavated underneath, are analyzed. Based on the measured data, a three-dimensional numerical analysis model considering the small strain hardening characteristics of soil is established, and the longitudinal deformation of buildings is studied. Some conclusions have been made here:

(1) The building with large aspect ratio and small foundation stiffness, the side near the shield develops "concave" deflection along the longitudinal direction, and the building foundation causes obvious spatial deformation. Simplifying it as a plane strain problem will underestimate the longitudinal deflection of buildings.

(2) There is a "lag effect" in the deformation caused by a shield passing parallelly alongside buildings according to the measured data. The building settlement tends to be stable after the shield tail leaves about 60 m away from the building. The settlement trough width coefficient of 0.5 would be suitable in analysis to describe the surface settlement. After shield tunneling, the maximum settlement of the longitudinal wall of the building is twice of its corner settlement.

(3) Considering the dual influence of building history and shield tunneling, the stress state of soil is complex. The development of soil stress above the shield axis affected by the construction history can be divided into six stages, and a process of loading−unloading−reloading is presented.

(4) Under the construction load, the soil beneath the center of the foundation on one side of the shield undergoes compression deformation caused by the increase of additional stress. The unloading deformation caused by stress release after the shield passing through occurs, resulting in the longitudinal “concave” deflection of the building.

(5) The interaction between the foundation and ground should be considered during the loading of construction, and it also determines the spatial deformation mode of foundation during the unloading stage of shield excavation. In the analysis, the longitudinal deflection caused by shield excavation will be significantly reduced, when the aspect ratio of building plane is less than 2.0.

Generally, the conclusions above are summarized based on the engineering background of this paper. The variation of superstructure forms, soil layer distribution, foundation stiffness and other factors affect the spatial deformation of buildings. Further investigation is required on those factors.

References

[1] ATTEWELL P B, YEATES J, SELBY A R. Soil

movements induced by tunnelling and their effects on pipelines and structures[M]. London: Blackie and Son Ltd., 1986.

[2] JIANG Xin-liang, JIA Yong, ZHAO Bao-jian, et al. Analysis of influence of metro tunnel construction on adjacent buildings[J]. Rock and Soil Mechanics, 2008, 29(11): 3047−3052.

[3] XIE Xiong-yao, ZHANG Yong-lai, ZHOU Biao, et al. Micro-settling control technology for shield tunnels crossing old buildings[J]. Chinese Journal of Geotechnical Engineering, 2019, 41(10): 1781−1789.

[4] SHE Xiang, YUAN Da-jun. Influence of shield pitch angle variation on shield-soil interaction[J]. Rock and Soil Mechanics, 2020, 41(4): 1366−1376.

[5] FARGNOLI V, BOLDINI D, AMOROSI A. TBM tunnelling-induced settlements in coarse-grained soils: the case of the new Milan underground line 5[J]. Tunnelling and Underground Space Technology, 2013, 38: 336−347.

[6] HOU Gong-yu, XIE Bing-bing, HAN Yu-chen, et al. Experimental study and engineering application of coupling performance between distributed embedded optical fiber and tunnel lining[J]. Rock and Soil Mechanics, 2020, 2020, 41(2): 714−726.

[7] LIU Chong-qing, ZENG Ya-wu, ZHU Ze-qi, et al. Study on ground surface settlement induced by shield tunneling in upper-soft and lower-hard ground in Xiamen[J]. Journal of Railway Science and Engineering, 2018, 15(2): 444−449.

[8] PECK R B. Deep excavations and tunnelling in soft ground[C]//Proceedings of the 7th International Conference on Soil Mechanics and Foundation Engineering. Mexico City: [s. n.], 1969: 225−290.

[9] RANKIN W J. Ground movements resulting from urban tunnelling: predictions and effects[C]//Proceedings of the 23rd Annual Conference of the Engineering Group of the Geological Society. Nottingham: Geological Society, 1988: 79−92.

[10] LU Ping, GENG Yan, ZHANG Wen-jun, et al. Study of influence of crossing mode of parallel tunnels on deformation of Masonry buildings[J]. Tunnel Construction, 2019, 39(1): 60−67.

[11] LU Xi-xi, JIAN Yun-qi, WANG Xian-ming, et al. Analysis on settlement characteristics of building foundation side ─ passed by shield tunnel in weak stratum[J]. Railway Standard Design, 2019, 63(12): 118−124.

[12] XU Li-hua, AI Xin-ying, YU Jia-li, et al. Analysis of impact of tunnel construction on masonry buildings in Xiamen airport road[J]. Chinese Journal of Rock Mechanics and Engineering, 2010, 29(3): 583−592.

[13] DING Zu-de, PENG Li-min, SHI Cheng-hua. Analysis of influence of metro tunnel crossing angles on ground buildings[J]. Rock and Soil Mechanics, 2011, 32(11): 3387−3392.

[14] HE Mei-de, LIU Jun, LE Gui-ping, et al. Study of impact of shield tunneling side-crossing on adjacent high buildings[J]. Chinese Journal of Rock Mechanics and Engineering, 2010, 29(3): 603−608.

[15] FRANZIUS J N. Behaviour of buildings due to tunnel induced subsidence[D]. London: Imperial College of Science, 2003.

[16] Ministry of Housing and Urban-Rural Development of the People's Republic of China. GB 50911－2013 Code for monitoring measurement of urban rail transit engineering[S]. Beijing: China Architecture & Building Press, 2013.

[17] Ministry of Housing and Urban-Rural Development of the People's Republic of China. GB 50652－2011 Code for risk management of underground works in urban rail transit[S]. Beijing: China Architecture & Building Press, 2011.

[18] Ministry of Housing and Urban-Rural Development of the People's Republic of China. GB50007－2011 Code for design of building foundation[S]. Beijing: China Architecture Building Press, 2011.

[19] WEI Gang. Selection and distribution of ground loss ratio induced by shield tunnel construction[J]. Chinese Journal of Geotechnical Engineering, 2010, 32(9): 1354−1361.

[20] CLAYTON C R I. Stiffness at small strain: research and practice[J]. Géotechnique, 2011, 61(1): 5−37.

[21] ZHENG Gang, LI Zhi-wei. Finite element analysis of responses of building adjacent to excavation considering initial differential settlement[J]. Rock and Soil Mechanics, 2012, 33(8): 2491−2499.

[22] LÜ Gao-feng, WEI Qing-chao, NI Yong-jun. Numerical analysis on the construction disturbance of shallow excavation tunnelling considering small strain behavior of soil[J]. China Railway Science, 2010, 31(1): 72−78.

[23] ATKINSON J H. Non-linear soil stiffness in routine design[J]. Géotechnique, 2000, 50(5): 487−508.

[24] O'REILLY M P, NEW B M. Settlements above tunnels in the United Kingdom-their magnitude and prediction[C]// Proceedings of Tunnelling 82. London: Institution of Mining and Metallurgy, 1982: 173−181.

[25] POTTS D M, ADDENBROOKE T I. A structure's influence on tunnelling-induced ground movements[J]. Proceedings of the ICE-Geotechnical Engineering, 1997, 125(2): 109−125.